Nuclear Science and Techniques (2023) 34:17
https://doi.org/10.1007/s41365-022-01155-2

Analysis of burnup performance and temperature coefficient for a small modular molten-salt reactor started with plutonium

Xue-Chao Zhao[1,2] · Yang Zou[1,2,3] · Rui Yan[1,2,3] · Xiang-Zhou Cai[1,2,3]

Received: 14 September 2022 / Revised: 26 October 2022 / Accepted: 14 November 2022 / Published online: 31 January 2023

Abstract

In a thorium-based molten salt reactor (TMSR), it is difficult to achieve the pure ^{232}Th–^{233}U fuel cycle without sufficient ^{233}U fuel supply. Therefore, the original molten salt reactor was designed to use enriched uranium or plutonium as the starting fuel. By exploiting plutonium as the starting fuel and thorium as the fertile fuel, the high-purity ^{233}U produced can be separated from the spent fuel by fluorination volatilization. Therefore, the molten salt reactor started with plutonium can be designed as a ^{233}U breeder with the burning plutonium extracted from a pressurized water reactor (PWR). Combining these advantages, the study of the physical properties of plutonium-activated salt reactors is attractive. This study mainly focused on the burnup performance and temperature reactivity coefficient of a small modular molten-salt reactor started with plutonium (SM-MSR-Pu). The neutron spectra, ^{233}U production, plutonium incineration, minor actinide (MA) residues, and temperature reactivity coefficients for different fuel salt volume fractions (*VF*) and hexagon pitch (*P*) sizes were calculated to analyze the burnup behavior in the SM-SMR-Pu. Based on the comparative analysis results of the burn-up calculation, a lower *VF* and larger *P* size are more beneficial for improving the burnup performance. However, from a passive safety perspective, a higher fuel volume fraction and smaller hexagon pitch size are necessary to achieve a deep negative feedback coefficient. Therefore, an excellent burnup performance and a deep negative temperature feedback coefficient are incompatible, and the optimal design range is relatively narrow in the optimized design of an SM-MSR-Pu. In a comprehensive consideration, $P = 20$ cm and $VF = 20\%$ are considered to be relatively balanced design parameters. Based on the fuel off-line batching scheme, a 250 MWth SM-MSR-Pu can produce approximately 29.83 kg of ^{233}U, incinerate 98.29 kg of plutonium, and accumulate 14.70 kg of MAs per year, and the temperature reactivity coefficient can always be lower than −4.0pcm/K.

Keywords Molten salt fuel · Incinerate plutonium · ^{233}U production · Temperature reactivity coefficient

1 Introduction

As one of the candidate reactor types of the fourth-generation reactor system, the thorium-based molten salt reactor (TMSR), which combines the advantages of thorium resource utilization and molten salt reactor, has several outstanding advantages in advanced nuclear fuel utilization [1, 2]. TMSRs with a thermal or fast-neutron spectrum can achieve desirable fissile fuel breeding, radioactive waste reduction, and proliferation resistance [3–7]. A growing number of studies are being carried out in many countries and institutions, and various conceptual designs of reactor types have been produced [8–10]. As the problem of plutonium accumulation in pressurized water reactors (PWRs) is receiving increasing attention, research on the use of salt reactors to burn plutonium or the use of

This work was supported by the Chinese TMSR Strategic Pioneer Science and Technology Project (No. XDA02010000), Shanghai Pilot Program for Basic Research-Chinese Academy of Science, Shanghai Branch (No. JCYJ-SHFY-2021-003), and the Chinese Academy of Sciences Special Research Assistant Funding Project.

✉ Yang Zou
zouyang@sinap.ac.cn

Xue-Chao Zhao
zhaoxuechao@sinap.ac.cn

[1] Shanghai Institute of Applied Physics, Chinese Academy of Sciences, Shanghai 201800, China

[2] CAS Innovative Academies in TMSR Energy System, Chinese Academy of Sciences, Shanghai 201800, China

[3] University of Chinese Academy of Sciences, Chinese Academy of Sciences, Beijing 100049, China

plutonium to drive ^{232}Th/^{233}U conversion has gradually intensified [11, 12]. The TMSR starts with plutonium to efficiently incinerate plutonium extracted from the PWR and produce ^{233}U for the pure thorium–uranium cycle [13, 14]. Another advantage of using plutonium and thorium as start-up fuels is that the ^{233}U produced can be separated from the spent fuel by fluorinated volatilization methods instead of large-scale centrifuges. Therefore, in addition to enriched uranium-started molten salt reactors, the study of the physical characteristics of the molten salt reactor started with plutonium is also very attractive.

There are several flexible fuel cycle methods for salt reactors, including the one-through mode driven by low-enriched uranium, thorium–uranium self-sustaining mode based on offline batch processing, and thorium–uranium proliferation mode based on online reprocessing. Online reprocessing thorium–uranium proliferation modes [1, 15, 16], such as the molten-salt breeder reactor (MSBR) and molten salt fast reactor (MSFR), can achieve 100% utilization of thorium resources, which is considered to be the ultimate mode of thorium–uranium circulation in molten salt reactors. However, online fuel processing is restricted because it is difficult to achieve the implementation of dry-processing technology in the short term. Therefore, the thorium–uranium self-sustained mode based on offline batch processing is considered a better transitional technical solution from the one-through mode to the online reprocessing mode.

In recent years, small modular reactors have attracted worldwide attention because of their simple design and construction, modular, passive safety, and nuclear non-proliferation [17–19]. Based on modularization and fuel salt reprocessing, a small modular thorium molten salt reactor can efficiently utilize thorium. Flexible and diverse fuel processing schemes can be developed for small modular thorium salt reactors, according to the different development maturities of modular and offline batch processing technologies, as well as different thorium utilization objectives. Japan's FUJI-U3 conceptual design adopts an offline batch fuel management mode with a fuel batch processing cycle of 7.5 years (2000 full power days). The online bubbling system is used to remove fission gas and insoluble fission products, and the fluorination volatilization method is used to remove the remaining fission products, which can realize the self-sustaining of ^{233}U [20]. Japan also designed a FUJI-Pu reactor with a thermal power of 250 MW. Compared with other FUJI reactors, it can burn plutonium and produce more ^{233}U during the same period [21]. A transatomic power molten salt reactor (TAP-MSR) that uses ZrH as the moderator can achieve a satisfactory plutonium incineration efficiency of more than 80% [22]. Many studies on MSFRs in France have shown that the plutonium incineration efficiency of the fast spectrum is higher than that of the thermal spectrum [12]. Other studies have suggested that if plutonium is used as the starting fuel to breed ^{233}U in a graphite-moderated thermal spectrum molten salt reactor, the incineration efficiency of plutonium can also exceed 80% [23]. Relevant research also shows that in a 150 MW small molten salt reactor with optimized design, the uranium production is about 16.0 kg/a and the transmutation rate of TRUs can achieve about 36.1 kg/a, which can effectively reduce the spent fuel containing TRUs [24]. Using plutonium as fission fuel in a small modular molten-salt reactor (SM-MSR) can not only achieve the consumption of plutonium from the discharge of the PWR but also realize the production of ^{233}U fuel, which is the starting fuel for the pure ^{232}Th/^{233}U cycle in a molten salt reactor. Meanwhile, if online fuel processing technology is not adopted, coupled with a higher neutron leakage rate, it is difficult for SM-MSRs to achieve higher neutron economy, satisfactory fuel conversion performance, and nuclear fuel sustainability [25]. Therefore, more optimized designs need to be carried out to realize an efficient utilization of the fissile material in a molten salt reactor started with plutonium.

In this study, a SM-MSR that does not rely on online fuel reprocessing and uses reactor-grade plutonium as the starting fuel was designed to achieve long-period thorium–uranium self-sustaining performance. Graphite assemblies with different hexagon sizes and fuel channel radii were analyzed to obtain their effects on the burnup performance and temperature feedback coefficients. To obtain more detailed rules, the neutron energy spectra, ^{233}U breeding capability, plutonium incineration, MA accumulation, and temperature reactivity coefficients were calculated and compared to describe the burnup and safety performance in a SM-MSR.

2 Methodology

2.1 Reactor description and modeling

The SM-MSR-Pu consists of an active zone, a graphite reflective layer, upper and lower fuel salt chambers, a descending ring chamber, a heat exchanger, an internal structural component, a control rod system, and a reactor container. A geometric description of the reactor core is shown in Fig. 1. The molten salt is mainly distributed in three parts: the center channel of each hexagonal graphite cell, the upper and lower chambers, the heat exchanger, and the pipes. The height and diameter of the core active zone are 3.2 m and 3.0 m, respectively, and the equivalent thickness of the upper and lower reflective layers is 20 cm. The B_4C layer with a thickness of 2 cm is mainly used to reduce the leakage of neutrons from the active zone, thus protecting the external structures from irradiation. The descending ring chamber, filled with fuel salt, is the downflow channel of the cooled fuel. The reactor

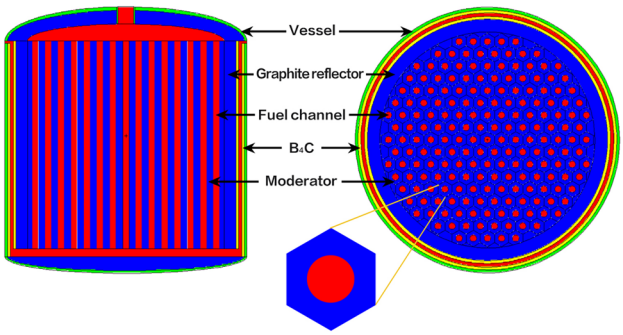

Fig. 1 (Color online) Geometrical description of the small modular molten-salt reactor (SM-MSR) core

container is made of Hastelloy material with a thickness of 3 cm. It wraps the entire structural body and serves as the primary circuit boundary. The fuel salt is heated by fission energy in the active zone, flows out of the core, and flows upward into the heat exchanger, transferring energy to the secondary circuit. Then, the fuel salt that flows out of the heat exchanger is collected into the lower chamber through the descending ring chamber, and finally returns to the active zone. The thermal power of the reactor is 250 MW and the electric power is 100 MW. Both the power and size of the core meet the current requirements for miniaturization and modularity. The composition of the fuel salt is 70%LiF+17.5%BeF_2+12.5%(ThF_4 +PuF_3), and the enrichment of Li-7 was 99.995%. The starting fuel plutonium is extracted from the spent fuel of a PWR , which consists of approximately 1.8% ^{238}Pu, 59% ^{239}Pu, 23% ^{240}Pu, 12.2% ^{241}Pu, and 4% ^{242}Pu [11]. The main reactor parameters are listed in Table 1.

An important advantage of salt reactors is that they can be coupled with flexible fuel reprocessing methods. During operation, a large amount of neutron poisons, such as fission products and minor actinides (MAs), accumulate in the fuel salt. To improve the neutron economy, neutron poisons must be regularly separated and removed from the fuel salt. The post-processing of the fuel salt is mainly divided into two parts: the bubbling system and the electrochemical separation system. The bubbling system is a processing method based on the physical separation of gases and liquids. Gaseous fission products and noble metals can be quickly removed by an online helium bubbling system with a very efficient separation rate [14]. Here, the separation period of the gaseous and noble metal fission products was set to 30 s, which is the same as that of the MSBR [1]. Electrochemical separation systems can separate soluble fission products (FPs) such as lanthanides or MAs, which cannot be separated by bubbling systems.

Table 1 Main parameters for the SM-MSR started with plutonium (SM-MSR-Pu)

Parameter	Value
Thermal power (MWth)	250
Core diameter (m)	3.54
Core height (m)	3.60
Fuel composition	LiF- BeF_2- (ThF_4+PuF_3)
Fuel (mol.fraction%)	70 -17.5 -12.5
Started fuel	Pu + Th
Feed fuel	Pu
Li-7 enrichment (mol%)	99.995
Thermal expansion (g/cm^3/K)	6.7×10^{-4}
Core life (year)	10
Height of active zone (m)	3.20
Diameter of active zone (m)	3.00
Thickness of side reflector (cm)	20
Thickness of upper/lower Chamber (cm)	20 / 20
Fuel channel number	To be optimized
Fuel channel radius (cm)	To be optimized
Fuel subassembly hexagon size (cm)	To be optimized

2.2 Methodology of the analysis

The online refueling scheme can allow for lower excess reactivity, achieve lower initial fissile fuel loadings, and simplify the reactor control requirements. Stabilizing k_{eff} and maintaining a critical state can easily be achieved through the coordination of the control rods and an online fuel refueling module. After each operation cycle of 10 years, the reactor container is replaced, and all the fuel salt is transported to the fuel-processing module for post-processing. In a modular molten-salt reactor, the fuel-processing module is a separate module. A reprocessing flowchart for the batch mode is shown in Fig. 2. In this scheme, dry reprocessing technologies such as fluorination volatilization, reductive extraction, and reduced pressure distillation are used to separate

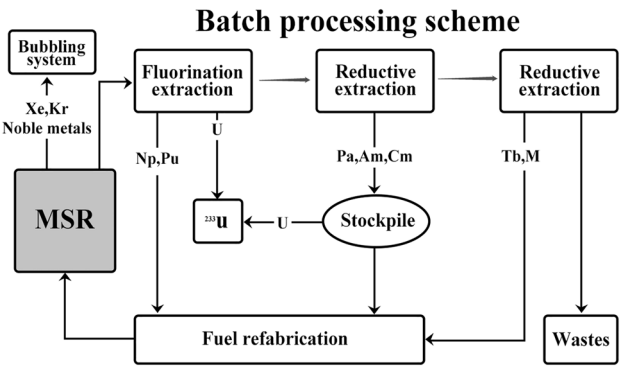

Fig. 2 Flowchart of reprocessing scheme

uranium, thorium, transuranic isotopes (TRUs), and fissile products (FPs) from the fuel salt. Uranium, neptunium, and plutonium are first extracted by fluorination and quickly reinjected into the core, while FPs and other radioactive nuclear wastes are processed and buried. ORNL's related experimental research shows that under suitable separation conditions using fluorinated extraction technology, the separation efficiency of uranium and neptunium can reach 99%, and that of plutonium can reach 90%. Reductive extraction technology can be used to separate thorium and other transuranic elements, and reduced-pressure distillation technology can be used to recover carrier salts. Coupled with fuel reprocessing and container equipment replacement every ten years, an SM-MSR can achieve continuous operation for multiple generations.

The TRITON program module in SCALE6.1 can complete the criticality and burnup calculation of solid-state reactors, but it cannot realize the functions of online fuel addition and on-line fission gas removal in salt reactors. To perform the burnup calculation for a MSR with on-line or off-line fuel reprocessing, a special MSR reprocessing sequence (MSR-RS) [26] has been developed in the previous work of our colleagues, which can simulate on-line refueling and batch processing for the SM-MSR-Pu. The MSR-RS program is coupled with the criticality analysis module (CSAS6) [27], problem-dependent cross section processing module (TRITON) [28], and depletion and decay calculation module (ORIGEN-S) in the SCALE6.1 program [29]. The TRITON module is used to perform critical calculations and generate the corresponding nuclide cross sections and neutron flux files, which provide the required single-group cross sections and neutron flux densities for the ORIGEN-S program calculations. The ORIGEN-S module is used to carry out the burnup calculation, in which on-line refueling and continuous gas removal are implemented by modifying the corresponding terms of the burnup equation, respectively. The CSAS module is used for critical analysis to judge the rationality of on-line refueling.

3 Results and discussion

3.1 Neutron spectrum and cross section

The neutron spectrum, which is mainly determined by the graphite moderation ratio, has a strong impact on the performance of the fissile material inventory, Th–U conversion capacity, and passive safety. For the hexagonal cell geometry, the moderation ratio can be controlled by changing both the fuel channel radius and hexagon pitch size. First, the ratio of the channel radius (R) to the hexagon pitch size determines the fuel salt volume fraction in the active zone. Second, for a certain VF, the hexagon P size determines the size of the graphite subassembly and thus affects the uniformity of the neutron moderation. Figure 3(left) shows the initial neutron spectra of different fuel salt volume fractions. It can be observed that the neutron spectrum hardens significantly with increasing VF owing to the reduction of the graphite moderator. When the fuel salt volume fraction is 5%, the neutron spectrum is mainly concentrated in the thermal spectrum. When the fuel salt volume fraction exceeds 20%, the flux of fast neutrons exceeds that of thermal neutrons. Moreover, ^{239}Pu and ^{240}Pu have obviously high capture cross sections near energies of 0.1 eV and 1.0 eV, respectively, leading to strong neutron absorption peaks and obvious depressions in the spectra.

Compared with the fuel volume fraction, the hexagon pitch size has a relatively small effect on the neutron

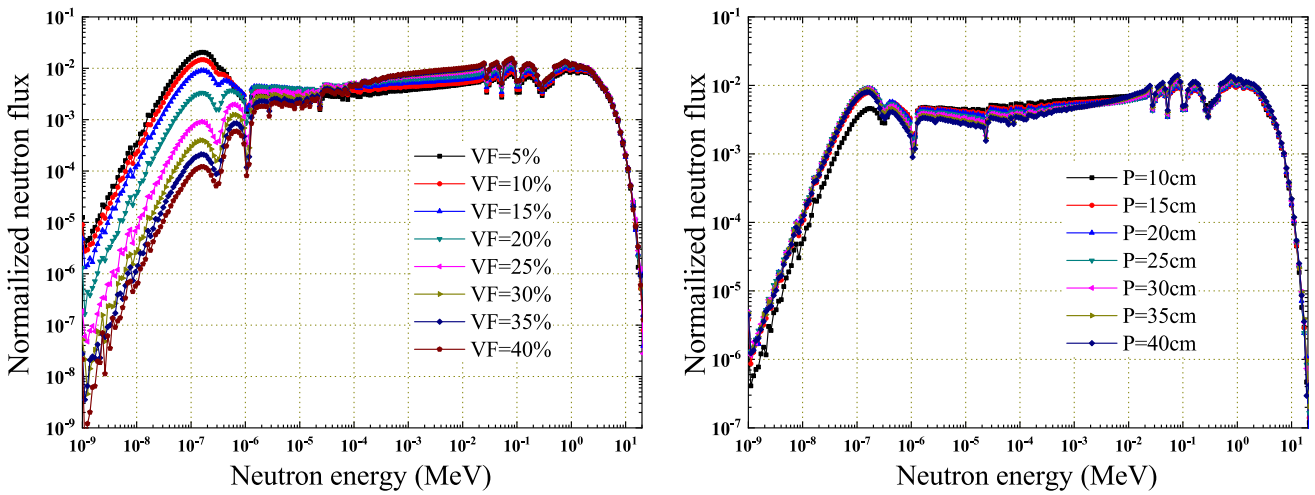

Fig. 3 (Color online) Initial neutron spectra for different fuel volume fractions (VF) (left) and different hexagon pitch (P) sizes (right)

spectrum, as shown in Fig. 3(right). The size of the hexagon P mainly affects the neutron-shielding effect. In the case of a larger P size, the neutron moderation is more inhomogeneous, so the neutron flux is relatively high in both the low- and high-energy regions, and the neutron flux in the middle energy region is low. For a smaller P size, the neutron moderation is more uniform and the neutron flux in the resonance energy region is higher, which will lead to larger resonance absorption near the 0.1 eV and 1.0 eV for ^{239}Pu and ^{240}Pu.

Plutonium is used as the fissile material, so its fission and capture cross section have a significant impact on the initial heavy metal (HM) mole fractions for criticality. For the same hexagon pitch size, the capture cross sections of all plutonium isotopes decrease with increasing fuel volume fraction. The fission cross sections of ^{239}Pu, ^{241}Pu, and^{238}Pu decrease with increasing fuel volume fraction, whereas the values of the other plutonium isotopes increase slightly with an increase in fuel volume fraction. The capture-to-fission ratio (α) is the ratio of the capture cross section to the fission cross section, and its change trend is the combined effect of the two cross-sectional changes of capture and fission. As shown in Fig. 4 (right), with an increase in fuel volume fraction, the capture-to-fission ratio of ^{239}Pu increases slightly, and the greater the hexagon pitch size, the smaller the capture-to-fission ratio.

The capture cross section of the plutonium isotopes showed an increasing trend with the increase in hexagon pitch size. The fission cross sections of ^{239}Pu and ^{241}Pu increased significantly, whereas the fission cross sections of other non-fissile isotopes remained basically unchanged. Therefore, the α of ^{239}Pu and ^{241}Pu remained unchanged, and the α values of the other nuclides increased with an increase in the hexagon pitch size. The influence of the fuel VF and P size on the initial plutonium loading molar fraction is shown in Fig. 4(left), and the evolution trend is similar to that of the α variation curve of plutonium. The main difference is that when $P = 5$ cm, the assembly size limits the thickness of the graphite moderator; thus, it cannot generate sufficient thermal neutrons. Therefore, its neutron spectrum is the hardest, and requires more plutonium loading. Furthermore, a larger volume fraction will lead to a faster neutron flux density and further harden the neutron spectrum, which will instead increase the fission cross section of ^{239}Pu. Therefore, the loading mole of plutonium decreased with an increase in volume fraction when volume fraction was greater than 20%.

Table 2 lists the micro cross sections and inventories of the main heavy nuclides after a 10-year operation. In this table, σ_f denotes the mean microscopic fission cross section. σ_c denotes the mean microscopic capture cross section. α is the ratio of σ_c to σ_f; TRUs with small α values, such as ^{239}Pu and ^{241}Pu, are favorable and can provide surplus neutrons to other TRUs, such as ^{237}Np, ^{238}Pu,^{241}Am, and ^{243}Am. These nuclei require at least two radiation capture (n, γ) reactions to be transformed into fissile nuclides. Consider the ^{237}Np reaction chain as an example.

$$^{237}\mathrm{Np}\xrightarrow{(n,\gamma)}{}^{238}\mathrm{Np}\xrightarrow{\beta}{}^{238}\mathrm{Pu}\xrightarrow{(n,\gamma)}{}^{239}\mathrm{Pu}\rightarrow\ldots$$

^{233}U with a lower α value is more advantageous in fuel utilization than ^{239}Pu, mainly due to its higher effective fission neutrons (η) and lower neutron radiation capture (n, γ) cross sections. In almost all neutron energy ranges, the η of ^{233}U is relatively high (greater than 2.0), and a higher η can provide more neutrons for fission reactions. In addition, the atomic weight of ^{233}U is much smaller than that of ^{239}Pu, and the reaction chain for conversion into MAs is longer. Furthermore, the capture cross section of ^{233}U ($\sigma_c = 4.33$) is much smaller than that of ^{239}Pu ($\sigma_c = 17.31$). This results in a significantly lower probability of converting ^{233}U into MAs and reduces the accumulation of radioactive nuclear waste. Therefore, it can

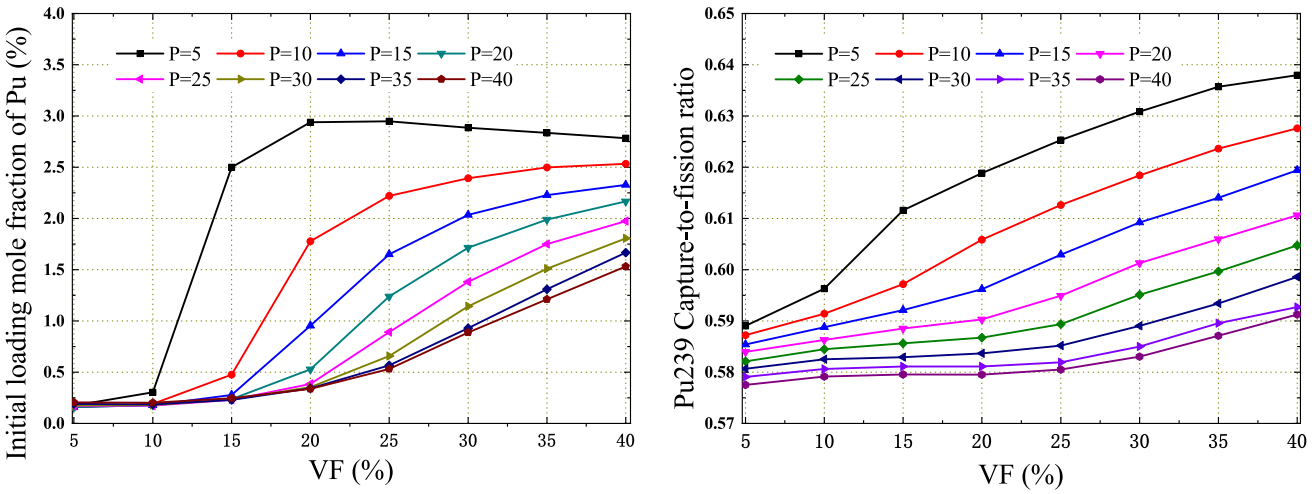

Fig. 4 (Color online) Initial loading mole fraction (left) and capture-to-fission ratio (right) of plutonium for different fuel volume fractions and hexagon pitch sizes

Table 2 Capture and fission cross sections and inventories of the heavy nuclei after 10-year operation

Nuclide	σ_c (barn)	σ_f (barn)	$\alpha(\sigma_c/\sigma_f)$	Inventory (kg)
^{232}Th	1.18	0.01	95.72	13230.00
^{231}Pa	29.93	0.18	166.09	0.58
^{233}Pa	22.20	0.04	524.55	4.89
^{232}U	6.43	14.01	0.46	0.27
^{233}U	4.33	26.44	0.16	302.80
^{234}U	17.90	0.32	56.25	26.33
^{235}U	5.89	14.74	0.40	5.72
^{236}U	10.44	0.26	40.91	0.63
^{238}U	8.99	0.05	169.65	0.00
^{237}Np	23.84	0.35	68.06	0.37
^{238}Pu	9.30	1.73	5.37	53.87
^{239}Pu	17.31	28.69	0.60	503.90
^{240}Pu	26.39	0.39	68.02	452.60
^{241}Pu	11.76	34.95	0.34	240.20
^{242}Pu	18.30	0.27	66.81	121.00
^{241}Am	43.62	0.55	78.87	49.59
^{243}Am	37.73	0.28	133.93	33.35
^{242}Cm	4.56	0.23	20.01	3.25
^{243}Cm	7.24	46.63	0.16	0.14
^{244}Cm	17.77	0.61	29.19	16.87

be concluded that the neutronic performance of ^{233}U is better than that of ^{239}Pu.

3.2 ^{233}U production

^{233}U production is directly determined by the ^{233}U accumulated inventory, which is closely related to the neutron absorption reaction rate of ^{232}Th and ^{233}U. The reaction chain for the evolution of ^{232}Th into ^{233}U is expressed as

$$^{232}\mathrm{Th} \xrightarrow{(n,\gamma)} {}^{233}\mathrm{Th} \xrightarrow{\beta} {}^{233}\mathrm{Pa} \xrightarrow{\beta} {}^{233}\mathrm{U}$$

For each generation of reactors, the net production of ^{233}U is the accumulation of ^{233}U in the fuel salt. At the end of the design life of each reactor, uranium, protactinium, and other actinides are extracted from the fuel salts and stored outside the core. Among them, almost all ^{233}Pa is converted to ^{233}U by (n,γ) decay with a half-life of 27 days. Therefore, the extracted ^{233}Pa should also be counted in the calculation of the breeding of ^{233}U. For multi-generation operating cycles, the total net ^{233}U production can be calculated by the addition of the ^{233}U inventory in the running reactor and the ^{233}U and ^{233}Pa extracted from the previous-generation reactor. The actual total ^{233}U production can be expressed as follows:

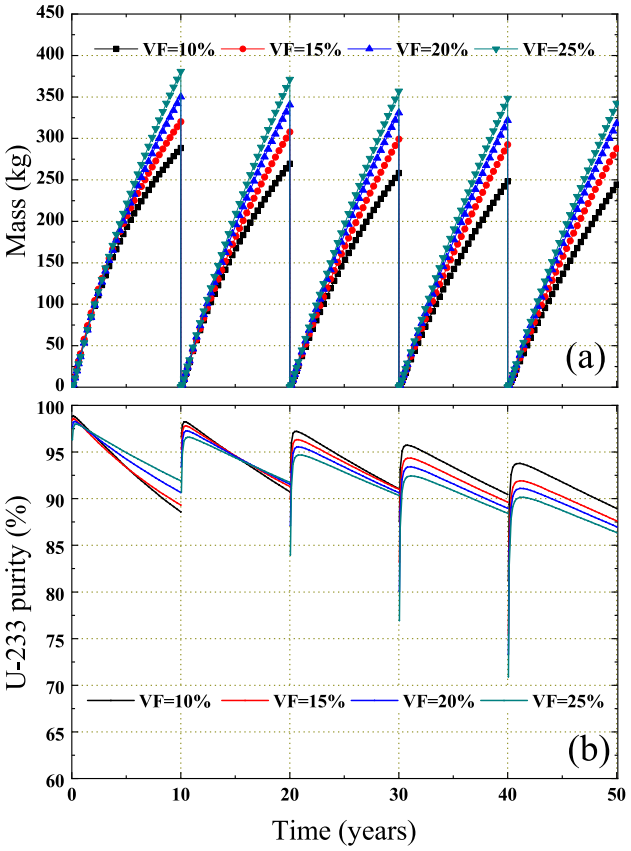

Fig. 5 (Color online) ^{233}U production and ^{233}U purity for different fuel salt volume fractions (P = 20 cm)

$$^{233}\mathrm{U(production)} = {}^{233}\mathrm{U(inventory)} + {}^{233}\mathrm{U(extract)} + {}^{233}\mathrm{Pa(extract)}, \quad (1)$$

where ^{233}U (inventory) refers to the residual ^{233}U inventory in the running reactor salt; ^{233}U (extract) and ^{233}Pa (extract) refer to the ^{233}U and ^{233}Pa extracted from the previous-generation reactor.

The ^{233}U inventories for different fuel volume fractions (P = 20 cm) during the 50-year reactor operation are shown in Fig. 5(a). With increasing fuel volume fraction, the neutron spectrum evidently hardens, and the difference between the neutron absorption reaction rate of ^{232}Th and ^{233}U continues to increase, resulting in a corresponding increase in ^{233}U production. In addition, ^{233}U production decreases slowly with the operating time, which is mainly due to the accumulation of TRUs and the consumption of thorium inventory. Further, ^{233}U production is not affected by the hexagon pitch size, which will not be discussed in detail here.

Plutonium and thorium are used as starting fuels and are not doped with uranium isotopes such as ^{235}U and ^{238}U; therefore, high-purity ^{233}U can be obtained by fluorination

extraction. Figure 5(b) shows the evolution of ^{233}U purity for different fuel volume fractions. In each refueling cycle of 10 years, the purity of ^{233}U decreases with operation time because of the accumulation of ^{234}U produced by the α decay of ^{238}Pu. Initially, the ^{233}U purity was the highest when the fuel volume fraction was 25%. However, the ^{233}U purity with $VF = 25\%$ decreased faster and was the lowest after 30 years.

In any case, ^{233}U purity can still be maintained above 85% during the 50-year operation, and the extracted ^{233}U can be used to start the pure thorium–uranium fuel cycle in future TMSRs.

3.3 Transuranic isotope (TRU) mole fraction

The molar fraction of the TRUs has an important impact on the long-term stable operation of the SM-MSR. The neutron energy spectrum, radiation intensity, and physicochemical properties of molten salt can be affected by the accumulation of TRUs.

To compensate for the reactivity loss, plutonium is continuously added to the fuel salt during the operation time, and the TRU molar fraction increases slowly. In addition, the accumulated uranium (mainly ^{233}U) is extracted from the fuel after a 10-year operation, and more fissile plutonium material is added to the next-generation core, causing a jump in the TRU molar fraction value. The TRU mole fractions for the different fuel volume fraction are shown in Fig. 6(a). It can be observed that the initial TRU molar fractions increase with the increase in fuel volume fraction owing to the harder neutron spectrum. After 10-year operation, the TRU molar fraction is approximately 4–10 times the initial value. Furthermore, a higher fuel volume fraction leads to a higher capture-to-fission ratio, lower neutron economy, and higher ^{233}U production, thereby requiring more plutonium feeding. For FLibe salt, the upper limit of TRU solubility is approximately 4%. After 50 years of operation, the TRU molar fractions for $VF = 20\%$ and $VF = 25\%$ increase to approximately 5% and 6%, respectively, both exceeding the upper limit solubility.

In theory, exceeding the upper solubility limit does not satisfy the stability of the physicochemical properties of molten salts. However, the MSR has the characteristic of fuel batch processing. In the actual operation process, when the TRU molar ratio reaches the upper limit of solubility, the salt can be post-processed to regenerate fresh fuel to ensure the chemical stability of the fuel salt.

The evolution of TRU molar fraction for different hexagon pitch sizes is shown in Fig. 6(b). As discussed in Sect. 3.1, the size of P mainly affects the neutron shielding effect. For a larger P size, neutron moderation is more inhomogeneous. The neutron flux is relatively high in both the low- and high-energy regions, whereas the neutron flux in the middle-energy region is low. Such a neutron energy distribution favors lower capture–fission ratios and better neutron economic performance, which is beneficial for reducing the accumulation of TRUs.

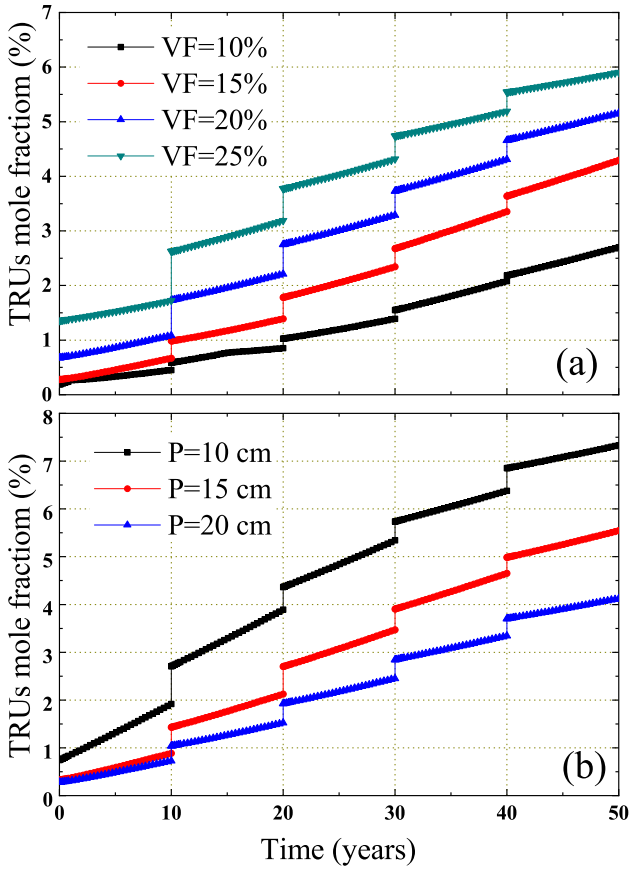

Fig. 6 (Color online) Transuranic isotope (TRU) mole fraction for different fuel salt volume fractions (P = 20 cm) and hexagon pitch sizes (VF = 15%)

Therefore, from the perspective of TRU molar fraction, a smaller fuel volume fraction and a larger hexagon pitch size are necessary to achieve long-term operation.

3.4 Plutonium incineration and minor actinide (MA) accumulation

Plutonium incineration depends on the fission contribution fraction of ^{233}U and the neutron absorption reaction rate of the plutonium isotopes.

The incineration of plutonium is inversely proportional to the fission contribution fraction of ^{233}U. ^{233}U production is completely separated from the fuel in each batch process, and its inventory is much smaller than that of plutonium, by approximately an order of magnitude. Therefore, the ^{233}U fission fraction is lower, and more fission reactions come from plutonium isotopes.

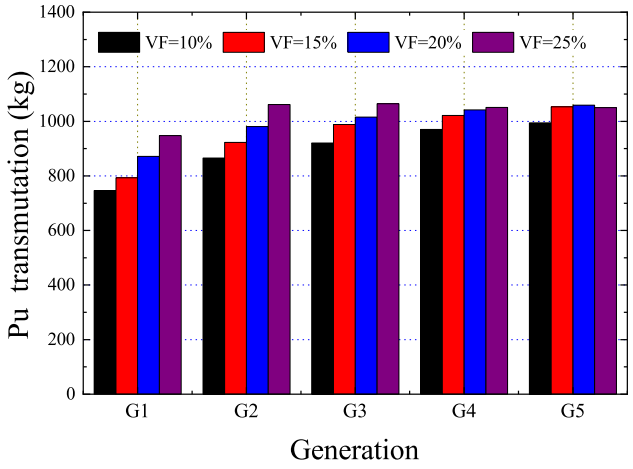

Fig. 7 (Color online) Plutonium incineration for different fuel salt volume fractions

The absorption reaction rates of plutonium isotopes increase with spectrum hardening owing to the larger capture–fission ratios of ^{239}Pu, ^{241}Pu, and ^{233}U. Larger capture–fission ratios indicate that more neutron capture is required for the same fission reaction rate. Therefore, the consumption of plutonium is higher under the same fission thermal power. As can be observed in Fig. 7, the annual plutonium incineration for the fuel volume fraction range (10%–25%) was approximately 70–105 kg/y.

Among all the isotopes of plutonium, the incineration rates of ^{239}Pu, ^{240}Pu, and ^{241}Pu are relatively high because of their higher neutron capture and fission cross sections. The incineration rates of ^{238}Pu and ^{242}Pu are relatively low because of their lower neutron absorption cross section and because of some key reaction chains, as follows:

$$^{241}\mathrm{Pu} \xrightarrow{\beta} {}^{241}\mathrm{Am} \xrightarrow{(\mathrm{n},\gamma)} {}^{242}\mathrm{Am} \xrightarrow{\beta} {}^{242}\mathrm{Cm} \xrightarrow{\alpha} {}^{238}\mathrm{Pu}$$

$$^{239}\mathrm{Pu} \xrightarrow{(\mathrm{n},\gamma)} {}^{240}\mathrm{Pu} \xrightarrow{(\mathrm{n},\gamma)} {}^{241}\mathrm{Pu} \xrightarrow{(\mathrm{n},\gamma)} {}^{242}\mathrm{Pu}$$

MAs are major long-lived high-level radioactive wastes, and their production should be minimized. The accumulation of MAs for different fuel volume fractions and hexagon pitch sizes is shown in Fig. 8. It can be observed that MA accumulation increases with an increase in fuel volume fraction and a decrease in the size of the hexagon P. This is mainly due to the higher initial plutonium mole fraction and higher capture-to-fission of TRUs for the higher fuel volume fraction and lower hexagon pitch size. During a 50-year operating period, the accumulated MA inventory reaches at least 400 kg.

For the $P = 20$ cm, $VF = 20\%$ case, the accumulation of MAs (mainly includes Np, Am, and Cm) increased to 103.57, 251.97, 401.70, 547.48, and 680.92 kg during the

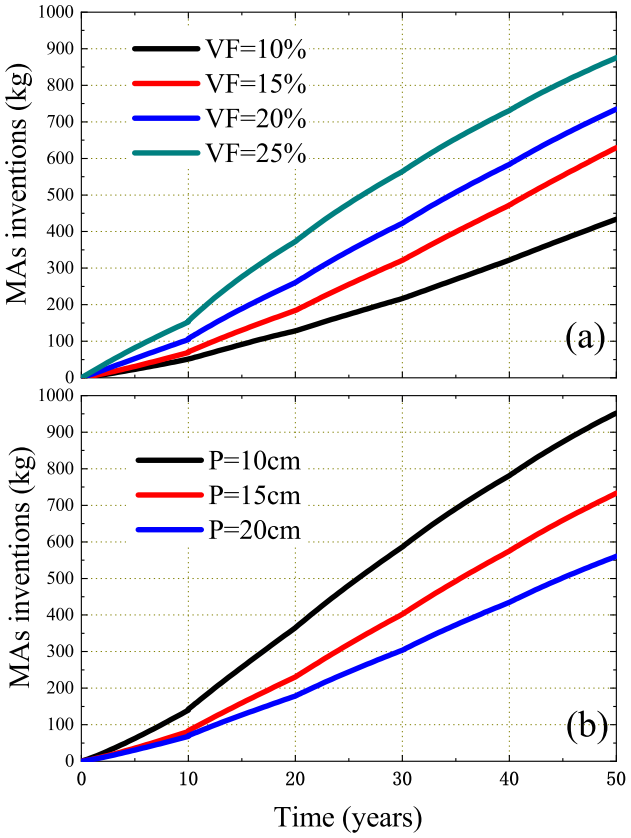

Fig. 8 (Color online) Minor actinide (MA) inventory for different fuel salt volume fractions ($P = 20$ cm) and hexagon pitch sizes ($VF = 15\%$)

five generations of the reactor, respectively. Among all the isotopes of MAs, the mass of ^{241}Am is the highest, mainly because of the higher β decay rate of ^{241}Pu. ^{237}Np is mainly derived from the α decay of ^{241}Amand the β decay of ^{237}U, shown as follows:

$$^{241}\mathrm{Pu} \xrightarrow{\beta(14.35\mathrm{years})} {}^{241}\mathrm{Am} \xrightarrow{(\mathrm{n},\alpha)} {}^{237}\mathrm{Np}$$

$$^{233}\mathrm{U} \xrightarrow{(\mathrm{n},\gamma)} {}^{234}\mathrm{U} \xrightarrow{(\mathrm{n},\gamma)} {}^{235}\mathrm{U} \xrightarrow{(\mathrm{n},\gamma)} {}^{236}\mathrm{U} \xrightarrow{(\mathrm{n},\gamma)}$$

$$^{237}\mathrm{U} \xrightarrow{\beta(6.75d)} {}^{237}\mathrm{Np}$$

It can be observed that the half-life of ^{241}Am (approximately 432.2 years) is relatively long, and the reaction chain for the conversion of ^{233}U to ^{237}Np involves four (n, γ) reactions; therefore, the production of ^{237}Np is limited in a certain period of time, and the inventory of neptunium is the lowest among all the main MAs.

Therefore, from the perspective of MA accumulation, a lower fuel volume fraction and larger hexagon pitch size are more beneficial for long-term operation and environmental compatibility, while a higher fuel volume fraction and lower hexagon pitch size are beneficial for plutonium incineration and ^{233}U production.

3.5 Temperature reactivity coefficient

The temperature reactivity coefficient is an important parameter for evaluating the passive safety features of reactors. To ensure the safe operation of the reactor, the temperature reactivity coefficient must have a negative value during the burnup process. For graphite-moderated salt reactors, the total temperature reactivity coefficient depends on the combined effect of the fuel and graphite. Therefore, the total feedback coefficient can be expressed as follows:

$$\left(\frac{\mathrm{d}k}{\mathrm{d}T}\right)_{\text{total}} = \left(\frac{\mathrm{d}k}{\mathrm{d}T}\right)_{\text{Doppler}} + \left(\frac{\mathrm{d}k}{\mathrm{d}T}\right)_{\text{density}} + \left(\frac{\mathrm{d}k}{\mathrm{d}T}\right)_{\text{graphite}} \quad (2)$$

where $(\mathrm{d}k/\mathrm{d}T)_{\text{Doppler}}$ represents the fuel Doppler effect, $(\mathrm{d}k/\mathrm{d}T)_{\text{density}}$ represents the fuel density fluctuation effect, and $(\mathrm{d}k/\mathrm{d}T)_{\text{graphite}}$ denotes the graphite effect.

The variation curve of the total temperature reactivity coefficient for different fuel volume fractions and hexagon pitch sizes at the start-up time is shown in Fig. 9. When the fuel volume fraction increases from 5% to 25%, the total temperature reactivity coefficients decrease significantly and can decrease from approximately 14 pcm/k to a negative value. For fuel volume fractions in the range of 10% to 25%, the total temperature reactivity coefficients are more obviously affected by the hexagon pitch size. In summary, a larger fuel volume fraction and smaller hexagon pitch size contribute more to a negative temperature reactivity coefficient.

The evolution trends of the fuel Doppler, fuel density, and graphite temperature coefficients with fuel volume fraction and hexagon pitch size are different.

The fuel Doppler coefficient is negative within the *VF* range of 10%–25%. For a *VF* less than 10%, the energy spectrum is softer, and the fission Doppler broadening of ^{239}Pu and ^{241}Pu caused by the temperature rise is more obvious; thus, the Doppler coefficient becomes a positive value. With an increase in fuel volume fraction, the energy spectrum becomes harder, the capture resonance contribution of other nuclides is obvious, and the Doppler coefficient becomes negative.

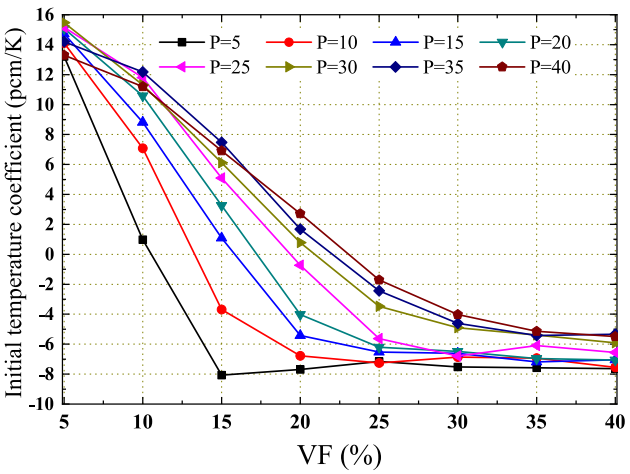

Fig. 9 Initial temperature reactivity coefficient for fuel salt volume fractions and hexagon pitch sizes

The fuel density coefficient is always positive for a fuel volume fraction less than 25%. As the temperature of the liquid fuel salt increases, the density drop caused by the expansion effect reduces the inventory of the fissile fuel within the active zone and softens the neutron energy spectrum. While the reduction of fissile nuclides can provide negative reactivity, the softening of the neutron spectrum will change the fission and capture cross sections of the main nuclides, which may lead to positive reactivity. For a fuel volume fraction less than 25%, the effect caused by the shift of the energy spectrum to the thermal neutron energy region is greater than the effect caused by the reduction in the fissile fuel, resulting in a positive value.

The graphite temperature coefficient decreases rapidly with an increase in the fuel volume fraction. For the range of neutron energy from 0.01 eV to 1 eV, the capture cross section of ^{232}Th is approximately inversely proportional to the neutron energy, whereas the fission cross section of ^{239}Pu and ^{241}Pu has a fission resonance peak between 0.02 eV and 0.04 eV. The influence of neutron spectrum hardening on the graphite temperature coefficient depends mainly on the competition between the capture reaction of ^{232}Th and the fission reactions of ^{239}Pu and ^{239}Pu. For a smaller volume fraction, the proportion of thermal neutrons is higher, and the increase in graphite temperature causes a shift in the neutron energy spectrum to ^{239}Pu and ^{241}Pu fission resonance peaks. This is more favorable for the fission reaction rates of ^{239}Pu and ^{241}Pu, resulting in increased reactivity and a positive graphite temperature coefficient. For a larger volume fraction, the neutron spectrum is relatively hard and deviated from the fission resonance peaks of ^{239}Pu and ^{241}Pu. The increase in the graphite temperature is more favorable for the ^{232}Th capture reaction, resulting in a negative graphite reactivity coefficient.

The temperature reactivity coefficients change continuously with the evolution of nuclides during the burnup process. The time evolution curves of the fuel Doppler, fuel density, and graphite temperature coefficients of (P = 20 cm VF = 20%) and (P = 20 cm VF = 15%) are shown in Fig. 10(a) and Fig. 10(b), respectively. For (P = 20 cm VF = 20%), the fuel Doppler temperature coefficient and graphite temperature coefficient are all negative and remain stable. The change in the total temperature reactivity coefficient mainly depends on the decrease in the fuel density coefficient. Different from VF = 20%, the graphite temperature coefficient of VF = 15% fluctuates greatly, it is 3.1 pcm/K

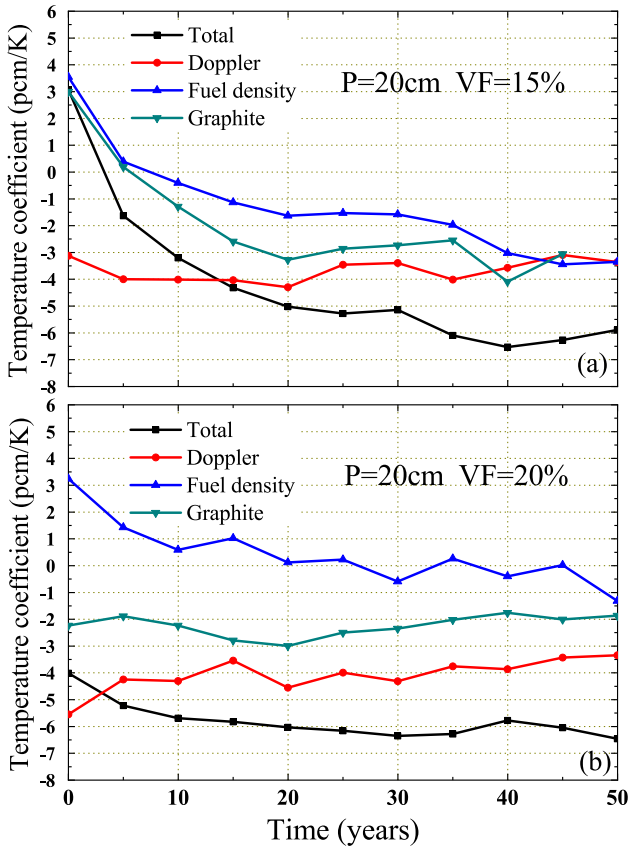

Fig. 10 Evolution of fuel Doppler, fuel density, and graphite temperature coefficients with burnup

at the initial moment, and approximately –4.1pcm/K after 40 years. The high graphite temperature coefficient value at the start-up time renders the design parameters of $P = 20$ cm $VF = 15\%$ unable to meet the requirements of passive safety.

In this study, the variations in the temperature reactivity coefficient with burnup time for different fuel volume fractions and hexagon pitch sizes were calculated. It was found that the overall trend of the total temperature reactivity coefficient declines throughout the burnup cycle. If the temperature coefficient at the initial moment is negative, then a negative reactivity coefficient can be achieved throughout the lifetime. Considering the requirements of inherent safety, thermal hydraulics, and control rod system design, the total temperature reactivity coefficient of the small modular TMSR must be less than –3.5pcm/K. From the previous results, it can be observed that increasing the fuel volume fraction and decreasing the hexagon pitch size can reduce the value of the total temperature reactivity coefficient. Therefore, the parameter ranges that satisfy the inherent safety constraints are: $P = 10$ cm ($VF \geq 15\%$), $P = 20$ cm ($VF \geq 20\%$), and $P = 30$ cm ($VF \geq 25\%$), and more detailed data is listed in table 3.

3.6 Burnup performance

The inventory curves of the main isotopes are shown in Fig. 11. During the 50-year burn-up process, approximately 380 kg of Th is consumed every 10 years, which is mainly converted into ^{233}Pa and further decays into ^{233}U. The stock of Pa rises rapidly, reaches an extremely high value in a short period of time, and decreases slightly with long-term burnup. The latter phenomenon is mainly due to the gradual decrease in the absorption reaction rate of ^{232}Th caused by hardening of the energy spectrum. The ^{233}U production in each refueling cycle also reduces gradually. During each 10-year refueling cycle, the mass of U rapidly accumulates to approximately 350 kg, and the purity of ^{233}U is approximately 85% or more. The uranium nuclides are then extracted from the cores using dry post-processing methods. Meanwhile, the extracted ^{233}Pa is stored outside the core for several months, decaying to ^{233}U. All these ^{233}U products can be used as starting fuels for other pure thorium–uranium cycle reactors.

The Pu inventory continues to increase throughout the operating period and remains the most stocked transuranic element, increasing from 821 to 5536 kg. The inventory of MA nuclides (Np, Am, and Cm) increases gradually, and the total mass is approximately 1/8 that of Pu. Among them, the mass of Am is the largest, mainly owing to the (n,γ) decay of ^{241}Pu. The inventory of Np is quite small, mainly because the (n,γ) decay of ^{237}U is the main method for generating ^{237}Np, whereas the yield of ^{237}U is extremely low in the Pu–Th fuel cycle.

The utilization and production of the main actinide nuclides during burnup are summarized in Table 4, in which the initial loading, cumulative feeding, inventory, net production, and net consumption are presented. It can be observed from the table that approximately 1.89 tons of thorium and 4.89 tons of plutonium were consumed, and 1.44 tons of ^{233}U was newly produced. During the five generations reactor, 302.8, 299.4, 290.0, 279.9, and 271.1 kg of ^{233}U were produced, and 817.22, 980.72, 1015.83, 1041.85, and 1058.97 kg of plutonium were incinerated, respectively. However, approximately 680.92 kg of MAs

Table 3 Design feasibility interval of fuel volume fraction and hexagon pitch satisfying the temperature reactivity coefficient

Hexagon pitch (P) sizes	5 cm	10 cm	15 cm	20 cm	25 cm	30 cm	35 cm	40 cm
Fuel salt volume fractions (VF)	≥ 12.5%	≥ 15%	≥ 18%	≥ 20%	≥ 23%	≥ 25%	≥ 27.5%	≥ 28.5%

Table 4 Fuel balance of SM-MSR-Pu in 50-year operation

Isotopes	^{232}Th	^{233}U	Pu	Minor actinides
Initial loading (kg)	13829.2	0	821.6	0
On-line feeding (kg)	0	0	9604.9	0
Separation-extraction (kg)	0	1172.1	0	0
Inventory (kg)	11940.0	271.1	5536.5	680.9
Net production(+) /consumption(–) (kg)	(–)1889.2	(+)1443.2	(–)4890.0	(+)680.9

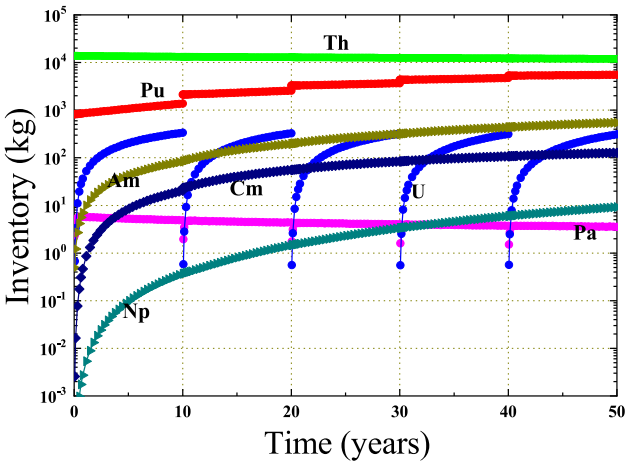

Fig. 11 (Color online) Evolution of actinide nuclides over time

were accumulated in the fuel salt at the end of the five generations reactor.

4 Conclusion

This study mainly focused on the burnup performance and passive safety features of a SM-MSR-Pu. Neutron energy spectra, ^{233}U breeding capability, plutonium incineration, MA accumulation, and temperature reactivity coefficients for different fuel volume fractions and hexagon pitch sizes were calculated and compared to describe the burnup and safety performance in the SM-MSR.

The results show that within the studied range (VF = 10%–40%) and P = (10–40 cm), a lower fuel volume fraction and a larger hexagon pitch size are more beneficial for neutron economy, long-term stable operation, and low radioactivity, whereas a higher fuel volume fraction and a lower hexagon pitch size are beneficial for plutonium incineration and ^{233}U production. Based on the comparative analysis results of the burn-up calculation, a lower volume fraction and larger pitch size are more beneficial for improving the burnup performance. The pursuit of a negative temperature reactivity coefficient limits the reactor design choices owing to passive safety requirements, and it turns out that a larger fuel volume fraction and smaller hexagon pitch size are necessary to achieve negative reactivity. For P = 10 cm, the fuel VF should be greater than 14% and for P = 20 cm, the volume fraction should be greater than 19% to ensure sufficient passive safety. Therefore, in the optimal design of the SM-MSR-Pu, the excellent fuel burn-up performance and deep negative temperature feedback coefficient are incompatible, and the optimal design range is relatively narrow.

A TMSR starts with plutonium and can be designed as a ^{233}U breeder, burning plutonium extracted from a PWR, and producing ^{233}U for the pure thorium–uranium cycle. For a comprehensive consideration, the parameters of P = 20 cm and VF = 20% were considered to be relatively balanced design parameters in this study. Based on the fuel off-line batching scheme, a 250 MWth SM-MSR-Pu can generate approximately 1.44 tons ^{233}U and incinerate 4.89 tons plutonium at the expense of accumulating 0.68 tons MAs in 50 years, and the temperature reactivity coefficient is always lower than –4.0pcm/K.

The performance analysis in this study mainly focused on the fuel cycle, and additional physical properties of the SM-MSR-Pu deserve further research in the future.

Acknowledgements All authors contributed to the study conception and design. Model design, simulation calculation and analysis were performed by Xue-Chao Zhao, Yang Zou and Rui Yan. Resources and supervision were performed by Yang Zou and Xiang-Zhou Cai. The first draft of the manuscript was written by Xue-Chao Zhao and all authors commented on previous versions of the manuscript. All authors read and approved the final manuscript.

References

1. R.C. Robertson, Conceptual design study of a single-fluid molten-salt breeder reactor. Oak Ridge National Lab., Tenn. (1971) https://doi.org/10.2172/4030941
2. M.W. Rosenthal, P.R. Kasten, R.B. Briggs, Molten-salt reactors-history, status, and potential. Nuclear Technol. **8**, 107–117 (1970)
3. A. Nuttin, D. Heuer, A. Billebaud et al., Potential of thorium molten salt reactors detailed calculations and concept evolution with a view to large scale energy production. Prog. Nucl. Energy. **46**, 77–99 (2005). https://doi.org/10.1016/j.pnucene.2004.11.001
4. D. LeBlanc, Molten salt reactors: A new beginning for an old idea. Nucl. Eng. Des. **240**, 1644–1656 (2010). https://doi.org/10.1016/j.nucengdes.2009.12.033

5. M.S. Cheng, Z.M. Dai, Development of a three dimension multi-physics code for molten salt fast reactor. Nucl. Sci. Tech. **25**, 010601 (2014). https://doi.org/10.13538/j.1001-8042/nst.25.010601
6. G.C. Li, Y. Zou, C.G Yu et al.,Influences of ^{7}Li enrichment on Th–U fuel breeding for an Improved Molten Salt Fast Reactor(IMSFR). Nucl. Sci. Tech. **28**, 97 (2017).https://doi.org/10.1007/s41365-017-0250-7
7. J. Křepel, B. Hombourger, C. Fiorina et al., Fuel cycle advantages and dynamics features of liquid fueled MSR. Ann. Nucl. Energy **64**, 380–397 (2014). https://doi.org/10.1016/j.anucene.2013.08.007
8. W.B. Cottrell, H.E. Hungerford, J.K. Leslie et al., Operation of the aircraft reactor experiment. No. ORNL-1845 (Del.). Oak Ridge National Lab.,Tenn., (1955) https://doi.org/10.2172/4237975
9. M. Brovchenko, J.L. Kloosterman, L. Luzzi et al., Neutronic benchmark of the molten salt fast reactor in the frame of the EVOL and MARS collaborative projects.EPJ Nuclear Sci. Technol., pp. 1–26(2019). https://doi.org/10.1051/epjn/2018052
10. P.N. Haubenreich, J.R. Engel, Experience with the molten salt reactor experiment. Nucl. Appl. Tech. 8, 118–136 (1970). https://doi.org/10.13182/nt8-2-118
11. M. Kütt, F. Friederike, M. Englert, Plutonium disposition in the BN-800 fast reactor: an assessment of plutonium isotopics and breeding. Sci. Glob. Secur. **22**, 188–208 (2014). https://doi.org/10.1080/08929882.2014.952578
12. E. Merle-Lucotte, D. Heuer, C. Le Brun et al.,Fast thorium molten salt reactors started with plutonium. Proceedings of ICAPP'06. American Nuclear Society, pp. 6132-6139 (2006)
13. D.Y. Cui, S.P. Xia, X.X. Li et al., Transition towards thorium fuel cycle in a molten salt reactor by using plutonium. Nucl. Sci. Tech. **28**, 152 (2017). https://doi.org/10.1007/s41365-017-0303-y
14. X.C. Zhao, D.Y. Cui, X.Z. Cai et al., Analysis of Th-U breeding capability for an accelerator-driven subcritical molten salt reactor. Nucl. Sci. Tech. **29**, 121 (2018). https://doi.org/10.1007/s41365-018-0448-3
15. D. Heuer, E. Merle-Lucotte, M. Allibert et al., Towards the thorium fuel cycle with molten salt fast reactors. Ann. Nucl. Energy **64**, 421–429 (2014). https://doi.org/10.1016/j.anucene.2013.08.002
16. G.C. Li, P. Cong, C.G. Yu et al., Optimization of Th-U fuel breeding based on a single-fluid double-zone thorium molten salt reactor. Prog. Nucl. Energy. **108**, 144–151 (2018). https://doi.org/10.1016/j.pnucene.2018.04.017
17. D.T. Ingersoll, Deliberately small reactors and the second nuclear era. Prog. Nucl. Energy **51**, 589–603 (2009). https://doi.org/10.1016/j.pnucene.2009.01.003.8
18. P. Sabharwall, E. Kim, M. Mckellar et al.,Small ModularMolten Salt Reactor (SM-MSR). ASME 2011 Small Modular Reactors Symposium, pp. 31–39 (2011).https://doi.org/10.1115/SMR2011-6527
19. Y. Ma, J. Chen, X. Cai et al., Preliminary quantitative proliferation resistance assessment of small modular thorium based MSR. Atomic Energy Science and Technology **52**, 1994–2000 (2018). https://doi.org/10.7538/yzk.2018.youxian.0162 (in Chinese)
20. K. Mitachi, T. Yamamoto, R. Yoshioka, Self-sustaining core design for 200 MWe molten-salt reactor with thorium-uranium fuel: FUJI-U3-(0). In: Proceedings of TU2007, pp. 4–6 (2007)
21. K. Mitachi, Y. Yamana, T. Suzuki et al., Neutronic examination on plutonium transmutation by a small molten-salt fission power station. No. IAEA-TECDOC–840.1995
22. B.R. Betzler, J.J. Powers, A. Worrall et al.,Two dimensional neutronic and fuel cycle analysis of the transatomic power molten salt reactor. Office of Scientific and Technical Information (OSTI), ORNL/TM- 2016/742.(2017). https://doi.org/10.2172/1340461
23. C.Y. Zou, C.Z Cai, C.G Yu et al.,Transition to thorium fuel cycle for TMSR. Nucl. Eng. Des. **330**, 420-428 (2018): https://doi.org/10.1016/j.nucengdes.2018.01.033
24. C.Y. Zou, C.G. Yu, G.F. Zhu et al., Neutronic performances of small modular thorium-based molten salt reactor starting with TRUs. Nucl. Tech. **43**(12), 120601 (2020). https://doi.org/10.11889/j.0253-3219.2020.hjs.43.120601 (in Chinese)
25. C.Y. Zou, X.Z. Cai, D.Z. Jiang et al., Optimization of temperature coefficient and breeding ratio for a graphite moderated molten salt reactor. Nucl. Eng. Des. **281**, 114–120 (2015). https://doi.org/10.1016/j.nucengdes.2014.11.022
26. C. Yu, C. Zou, J. Wu et al., Development and verification of molten salt reactor refueling and reprocessing system analysis code based on SCALE. Atomic Energy Science and Technology **52**, 12 (2018). https://doi.org/10.7538/yzk.2018.youxian.0123 (in Chinese)
27. ORNL, CSAS6:control module for enhanced criticality safety analysis with KENOVI. ORNL/TM-2005/39, Version 6.1. (2011)
28. M.D. DeHART, Triton:a two dimensional transport and depletion module for characterization of spent nuclear fuel. ORNL/TM-2005/39, Version 6.1. (2011)
29. Scale:a comprehensive modeling and simulation suite for nuclear safety analysis and design. ORNL/TM-2005/39, Version6.1. (2011)